

PROBING QCD IN LOW ENERGY $\bar{p}p$ COLLISIONS*

STANLEY J. BRODSKY

*Stanford Linear Accelerator Center
Stanford University, Stanford, California, 94305*

1. Introduction

A primary focus of study in particle and nuclear physics is the testing of quantum chromodynamics.¹ Although it is generally believed that QCD is the fundamental theory of the strong interactions, quantitative tests have so far been restricted to the high momentum transfer domain where perturbative methods based on asymptotic freedom can be used. Tests of the confining non-perturbative aspects of the theory are either quite qualitative or at best indirect.

An important question for the proposed AMPLE facility is whether studies of low to moderate energy antiproton reactions with laboratory energies under 10 GeV could give further insights into the full structure of QCD. As I shall argue in this talk, there are a number of exclusive and inclusive \bar{p} reactions which could provide useful constraints or test novel features of QCD in the intermediate momentum transfer domain involving both perturbative and non-perturbative dynamics.

* Work supported by the Department of Energy, contract DE - AC03 - 76SF00515.

2. High Momentum Transfer Reactions

The main testing ground of QCD over the past decade has been the domain of inclusive reactions at high momentum transfer. More recently we have learned how to develop perturbative predictions for high momentum transfer exclusive processes in which detailed features of hadron wavefunctions and amplitude coherence enter.²⁻⁶ Many of these predictions are directly applicable to antiproton-initiated reactions.

QCD has two essential properties which make calculations of processes at short distance or high momentum transfer tractable and systematic. The critical feature is asymptotic freedom: the effective coupling constant $\alpha_s(Q^2)$ which controls the interactions of quarks and gluons at momentum transfer Q^2 vanishes logarithmically at large Q^2 . Complementary to asymptotic freedom is the existence of factorization theorems for both exclusive and inclusive processes at large momentum transfer. In the case of exclusive processes (in which the kinematics of all the final state hadrons are fixed at large invariant mass), the hadronic amplitude can be represented as the product of a hard-scattering amplitude for the constituent quarks convoluted with a distribution amplitude for each incoming or outgoing hadron.²⁻⁶ (See Appendix A). The distribution amplitude contains all of the bound-state dynamics and specifies the momentum distribution of the quarks in the hadron.² The hard scattering amplitude can be calculated perturbatively as a function of $\alpha_s(Q^2)$. The analysis can be applied to form factors, exclusive photon-photon reactions, photoproduction, fixed-angle scattering, *etc.* In the case of the simplest processes, $\gamma\gamma \rightarrow M\bar{M}$ and the meson form factors, rigorous all-order proofs can be given.

The predictions of perturbative QCD have been strikingly confirmed in inclusive e^+e^- and $\gamma\gamma$ collisions, deep inelastic lepton reactions, massive lepton pair production, and the whole array of large p_T jet and photon reactions. Measurements of exclusive processes at high momentum transfer, especially form factors and two-body photon-photon reactions have led to detailed checks on the scaling

behavior of the theory. Recent results⁷ for $\gamma\gamma \rightarrow M\bar{M}$ are shown in fig 1. In general, the experimental results on the scaling behavior of exclusive and inclusive reactions appear consistent with short distance subprocesses based on the elementary scattering of spin 1/2 quarks and spin 1 gluons, the fundamental degrees of freedom of QCD.

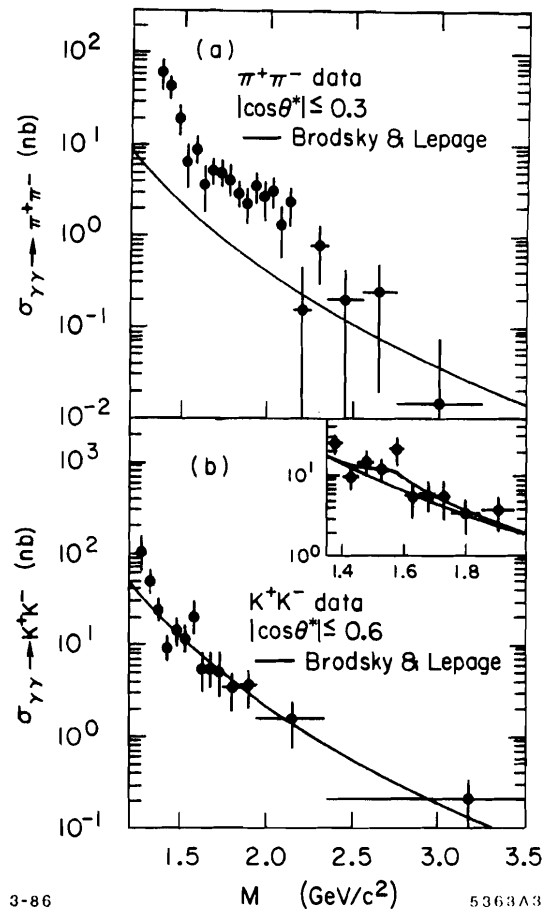


Fig. 1. Comparison of $\gamma\gamma \rightarrow \pi^+\pi^-$ and $\gamma\gamma \rightarrow K^+K^-$ meson pair production data with the parameter free perturbative QCD prediction of ref 2. The data are from ref 7.

The central unknown in the QCD predictions at this time is the composition of the hadrons in terms of their quark and gluon quanta.^{2,8} Recently, several important tools have been developed which allow specific predictions for the

hadron wave functions. A primary tool is the use of light-cone quantization to construct a consistent relativistic Fock state basis for the hadrons and their observables in terms of quark and gluon quanta. The distribution amplitudes and the structure functions are defined directly in terms of these light-cone wave functions.² The form factor of a hadron can be computed exactly in terms of a convolution of initial and final light-cone Fock state wave functions.⁹

Another important tool is the use of QCD sum rules to provide constraints on the moments of hadron distribution amplitudes.⁴ This method has yielded some information on the momentum space structure of mesons which we review in Appendix B. A particularly important challenge relevant to antiproton exclusive processes is the construction of baryon distribution amplitudes. Using the sum rule method, Chernyak and Zhitnitsky⁴ have proposed a model form for the nucleon distribution amplitude which together with the QCD factorization formulae, predict the correct sign and magnitude as well as scaling behavior of the proton and neutron form factors.¹⁰ (See fig. 2.)

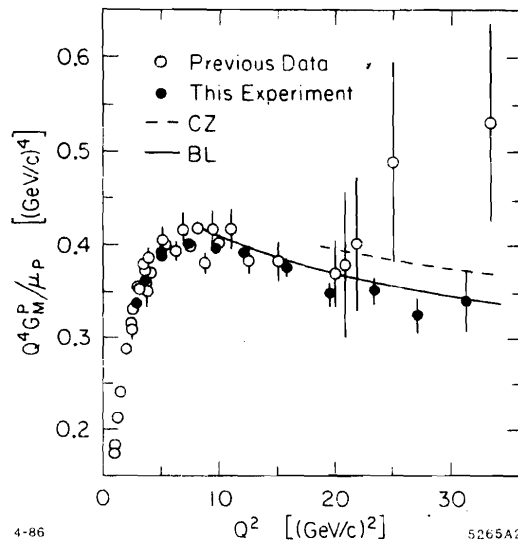


Fig. 2. Comparison of the scaling behavior of the proton magnetic form factor with the theoretical predictions of refs. 2 and 4. The CZ predictions⁴ are normalized in sign and magnitude. The data are from ref. 10.

Another recent advance has been the calculation of the moments of distribution amplitudes using lattice gauge theory.¹¹ The initial results are interesting – suggesting a highly structured oscillating momentum-space valence wave function for the meson. The results from both the lattice calculations and QCD sum rules demonstrate that the light quarks are highly relativistic in the bound state. This gives further indication that while non-relativistic potential models are useful for enumerating the spectrum of hadrons (because they express the relevant degrees of freedom), they are not reliable in predicting wave function structure.

3. Inclusive \bar{p} Reactions and the QCD Critical Length

The factorization structure of QCD implies that the structure functions and distribution amplitudes that control high momentum transfer reactions are process independent. The proofs are highly non-trivial. In the case of inclusive massive lepton-pair production (The Drell-Yan process), the $\bar{p}p \rightarrow \ell\bar{\ell}X$ cross section to leading order in $1/Q^2$ takes the form (see fig. 3):

$$\frac{d\sigma}{dx_a dx_b d\Omega} = \frac{1}{3} \sum_{q\bar{q}} G_{\bar{q}/\bar{p}}(x_a, Q) G_{q/p}(x_b, Q) \frac{d\sigma}{d\Omega}(q\bar{q} \rightarrow \mu^+\mu^-).$$

This factorization separates the long distance (non-perturbative) dynamics contained in the universal-process independent structure functions $G_{q/p} = G_{\bar{q}/\bar{p}}$ from the short-distance perturbative physics contained in the subprocess $q\bar{q} \rightarrow \mu^+\mu^-$ cross section. Antiproton tests of this classic QCD prediction are crucial since the beam and target structure functions for the valence quark and antiquarks are measured directly in deep inelastic lepton scattering.

Despite the simple form of the inclusive cross section, all-orders factorization for the Drell-Yan process has only just recently been analyzed to all orders in perturbation theory (by G. Bodwin¹² and J. Collins, D. Soper and G. Sterman.¹³) The most serious complications are due to the elastic and inelastic initial state hadronic interactions which potentially could affect the color correlations, and

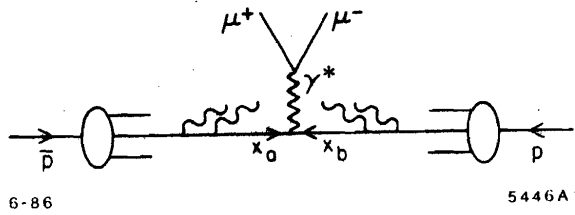


Fig. 3. Schematic representation of factorization of the Drell-Yan cross section in QCD.

momentum distribution of the annihilating q and \bar{q} .¹⁴ (see fig. 4) Clearly such effects ruin factorization in a macroscopic target. In fact, as shown in ref. 17 a necessary condition to eliminate the initial state effects is that the incident parton energy must be large compared to a scale proportional to the length of the target. This translates into a necessary condition for factorization:

$$Q^2 = M_N L \mu^2 / x_b$$

For a uranium target this implies that factorization can only be valid if the lepton pair mass is greater than a few GeV at large x_b . It is clearly interesting to study this phenomena experimentally, since it involves the transition between perturbative and soft dynamics and the propagation of antiquarks in nuclear matter. This important area of physics could be studied systematically using a low to medium energy \bar{p} beam.

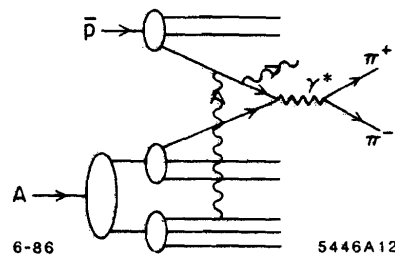


Fig. 4. Induced radiation from the interaction of the active antiquark with target spectators in the Drell-Yan process. The inelastic interactions are suppressed at parton energies which are large compared to a scale set by the length of the target.¹⁴

It should be noted that the factorization proofs have not yet been extended to reactions such as $p\bar{p} \rightarrow \text{Jet} + \text{Jet} + X$ where the subprocess channel is not in a color singlet. In addition, due to infrared noncancellations, factorization is known to break down beyond leading twist.¹⁵

4. QCD Predictions for $\bar{p}p$ Exclusive Processes

Dimensional counting rules¹⁶ give a direct connection between the degree of hadron compositeness and the power-law fall of exclusive scattering amplitudes at fixed center of mass angle: $M \sim Q^{4-n} F(\theta_{cm})$ where n is the minimum number of initial and final state quanta. This rule gives the QCD prediction for the nominal power law scaling, modulo corrections from the logarithmic behavior of α_s , the distribution amplitude, and small power-law corrections from Sudakov-suppressed Landshoff multiple scattering contributions. A brief introduction to these topics is given in Appendix A. For $\bar{p}p$ one predicts

$$\frac{d\sigma}{d\Omega} (\bar{p}p \rightarrow \gamma\gamma) \simeq \frac{\alpha^2}{(p_T^2)^5} f^{\gamma\gamma}(\cos\theta, \ln p_T)$$

$$\frac{d\sigma}{d\Omega} (\bar{p}p \rightarrow \gamma M) \simeq \frac{\alpha^2}{(p_T^2)^6} f^{\gamma M}(\cos\theta, \ln p_T)$$

$$\frac{d\sigma}{d\Omega} (p\bar{p} \rightarrow M\bar{M}) \simeq \frac{1}{(p_T^2)^7} f^{M\bar{M}}(\cos\theta, \ln p_T)$$

$$\frac{d\sigma}{d\Omega} (p\bar{p} \rightarrow B\bar{B}) \simeq \frac{1}{(p_T^2)^9} f^{B\bar{B}}(\cos\theta, \ln p_T)$$

The angular dependence reflects the structure of the hard scattering perturbative T_H amplitude, which in turn follows from the flavor pattern of the contributing duality diagrams. For example, a minimally connected diagram such as that illustrated in fig. 5 is approximately characterized¹⁷ as

$$T_H \sim \frac{1}{t^2} \frac{1}{s} \frac{1}{u}.$$

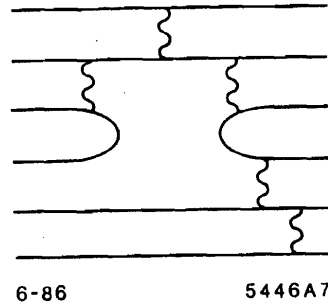


Fig. 5. A perturbative contribution to the hard scattering amplitude in nucleon-nucleon collisions.

We emphasize that comparisons between channels related by crossing of the Mandelstam variables places a severe constraint on the angular dependence and analytic form of the underlying QCD exclusive amplitude. For example, it is possible to measure and compare

$$\bar{p}p \rightarrow \gamma\gamma : \gamma p \rightarrow \gamma p : \gamma\gamma \rightarrow \bar{p}p$$

$$\bar{p}p \rightarrow \gamma\pi^0 : \gamma p \rightarrow \pi^0 p : \pi^0 p \rightarrow \gamma p .$$

SLAC measurements¹⁸ of the $\gamma p \rightarrow \pi^+ n$ cross section at $\theta_{CM} = \pi/2$ are consistent with the normalization and scaling (see fig. 6)

$$\frac{d\sigma}{dt} (\gamma p \rightarrow \pi^+ n) \simeq \frac{1 \text{ nb}}{(s/10 \text{ GeV})^7} f(t/s) .$$

We thus expect similar normalization and scaling for $\frac{d\sigma}{dt} (\bar{p}p \rightarrow \gamma\pi^0)$; all angle measurements up to $s \lesssim 15 \text{ GeV}^2$ appear possible given a high luminosity \bar{p} beam.

Extensive measurements¹⁷ of the $pp \rightarrow pp$ cross section have been made at ANL, BNL and other laboratories. The fixed angle data on a log-log plot (see fig. 7) appears consistent with the nominal $s^{-10} f(\theta_{CM})$ dimensional counting production. However, as emphasized by Hendry,¹⁹ the $s^{10} d\sigma/dt$ cross section

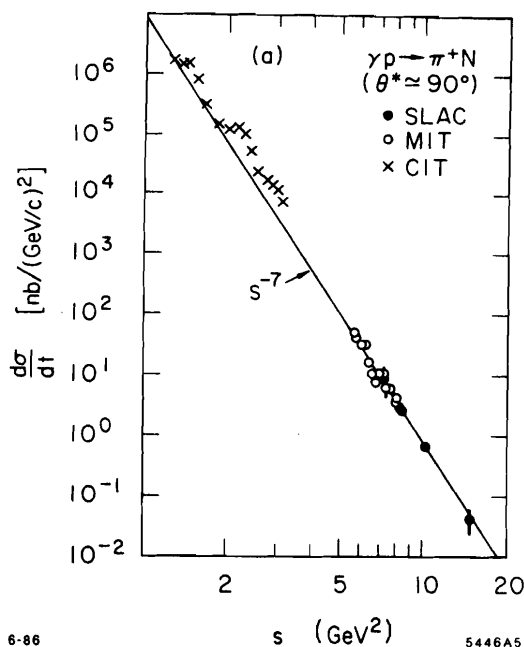


Fig. 6. Comparison of photoproduction data with the dimensional counting power-law prediction. The data are summarized in ref. 18.

exhibits oscillatory behavior with p_T . Even more serious is the fact that polarization measurements²⁰ show significant spin-spin correlations (A_{NN}), and the single spin asymmetry (A_N) is not consistent with predictions based on hadron helicity conservation (see sec. 6) which is expected to be valid for the leading power behavior.²¹ Recent analyses of these effects have been given by Farrar²² and Lipkin.²³ It is likely that there are significant non-leading power law contributions. in the accessible energy range. Clearly, $\bar{p}p \rightarrow \bar{p}p$ data in the large-angle large-energy regime will be very helpful in clarifying these fundamental issues.

The simplest exclusive channels accessible to a $\bar{p}p$ facility are $\bar{p}p \rightarrow e^+e^-$, $\mu^+\mu^-$, $\tau^+\tau^-$ which to leading order in α provides a direct measurement of the Dirac and Pauli timelike proton form factor. The θ_{CM} angular dependence can be used to separate F_2 and F_1 and check the basic prediction,²

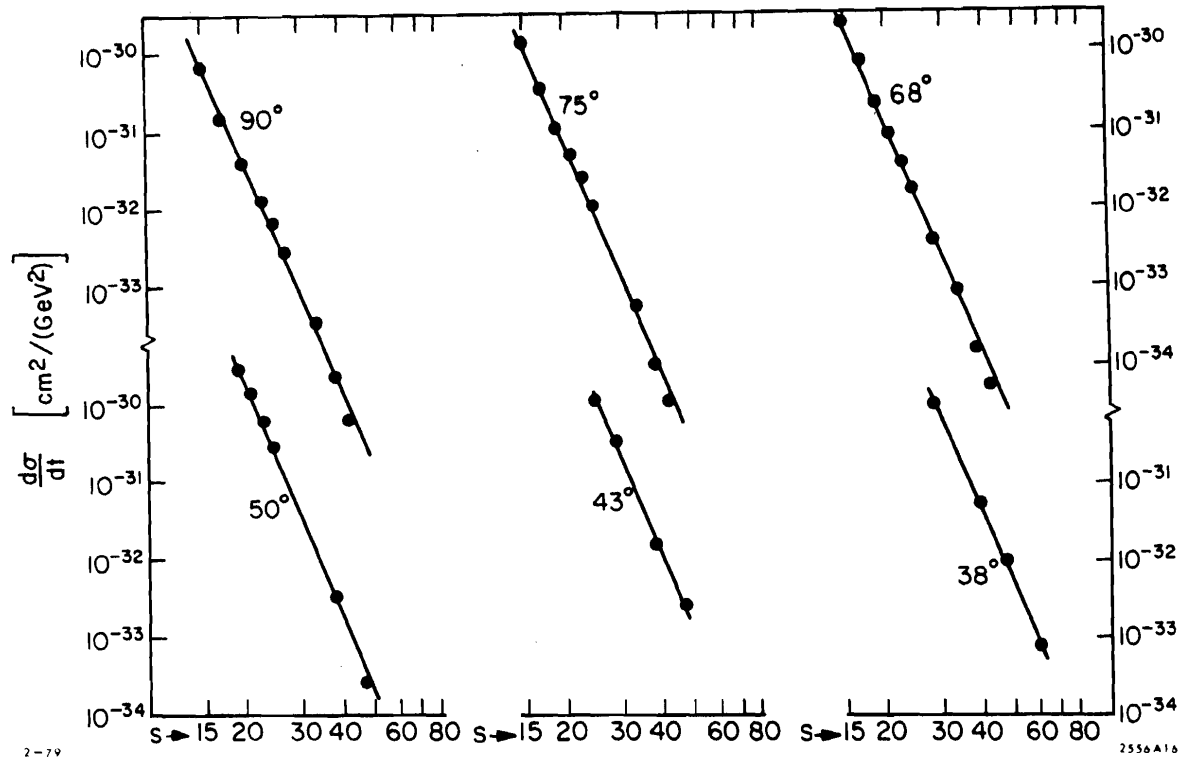


Fig. 7. Comparison of proton-proton scattering at fixed θ_{cm} with the dimensional counting prediction. The best fit is $s^{-9.7}$. See ref. 18.

$$F_2(s)/F_1(s) \sim M^2/s.$$

Perturbative QCD predicts asymptotic scaling of the form²

$$s^2 F_1(s) \sim f(\ln s).$$

A high luminosity \bar{p} facility could push timelike measurements of both form factors well beyond those available from e^+e^- storage rings. Since the normalization is similar to that of $p\bar{p} \rightarrow \gamma\gamma$, one should be able to measure the proton form factors out to center of mass energy squared as large as $s \sim 10 \text{ GeV}^2$.

5. Studying the Compton Amplitude in $p\bar{p}$ Annihilation

An important example of an exclusive process in QCD is the process $p\bar{p} \rightarrow \gamma\gamma$ as illustrated in fig. 8. Applying the procedure outlined in Appendix A, we can write to leading order in $1/p_T^2$,

$$\begin{aligned} \mathcal{M}_{p\bar{p} \rightarrow \gamma\gamma}(p_T^2, \theta_{CM}) &= \int_0^1 [dx] \int_0^1 [dy] \phi_{\bar{p}}(x, p_T) \\ &\times T_H(qqq + \bar{q}\bar{q}\bar{q} \rightarrow \gamma\gamma) \phi_p(y, p_T) \end{aligned}$$

where $\phi_p(x, p_T)$ is the antiproton distribution amplitude and $T_H \sim \alpha_s^2(p_T^2)/(p_T^2)$ gives the scaling behavior of the minimally connected tree graph amplitude for the two-photon annihilation of three quarks and three antiquarks collinear with the initial hadron directions. (See fig. 9.) QCD thus predicts

$$\frac{d\sigma}{d\Omega_{CM}}(p\bar{p} \rightarrow \gamma\gamma) \simeq \frac{\alpha_s^4(p_T^2)}{(p_T^2)^5} f(p_T, \theta_{CM}, \ln p_T^2).$$

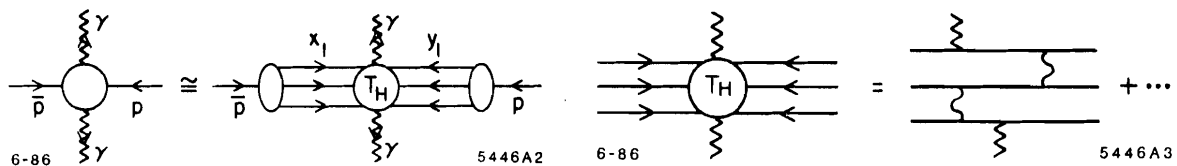


Fig. 8. Application of QCD factorization to $\bar{p}p$ annihilation into photons.

Fig. 9. Example of a lowest order perturbative contribution to T_H for the process $\bar{p}p \rightarrow \gamma\gamma$.

The complete calculations of the tree graph structure (see figs. 10-12) of both $\gamma\gamma \rightarrow M\bar{M}$ and $\gamma\gamma \rightarrow B\bar{B}$ amplitudes has now been completed. One can use crossing to compute T_H for $p\bar{p} \rightarrow \gamma\gamma$ to leading order in $\alpha_s(p_T^2)$ from the calculations reported by Farrar, Maina, and Neri²⁴ and Gunion and Millers.²⁵

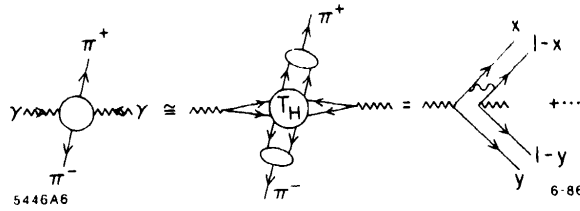


Fig. 10. Application of QCD to two photon production of meson pairs.²⁸

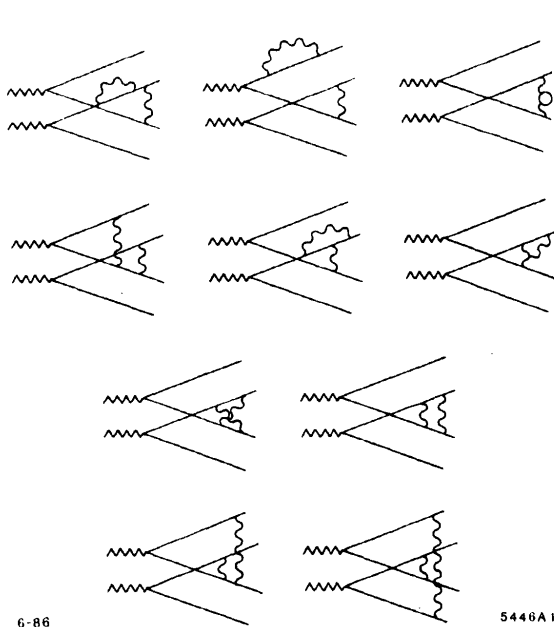


Fig. 11. Next to leading perturbative contribution to T_H for the process $\gamma\gamma \rightarrow MM$. The calculation has been done by Nizic.²⁸

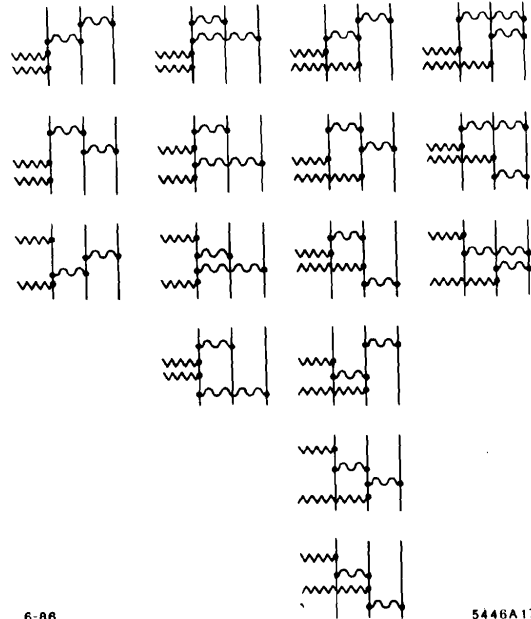


Fig. 12. Leading diagrams for $\gamma + \gamma \rightarrow \bar{p} + p$ calculated in refs. 24, 25.

Examples of the predicted angular distributions are shown in figs. 13 and 14. The region of applicability of the leading power-law results is presumed to be set by the scale where $Q^4 G_M(Q^2)$ is roughly constant, i.e.: $Q^2 > 3 \text{ GeV}^2$. (See fig. 2.) Preliminary two photon collision measurements²⁶ (for energies too close to the $\bar{p}p$ threshold) are shown in fig. 15. As discussed in Appendix B, a model form for the proton distribution amplitude has been proposed by Chernyak and Zhitnitskii⁴ based on QCD sum rules which leads to normalization and sign consistent with

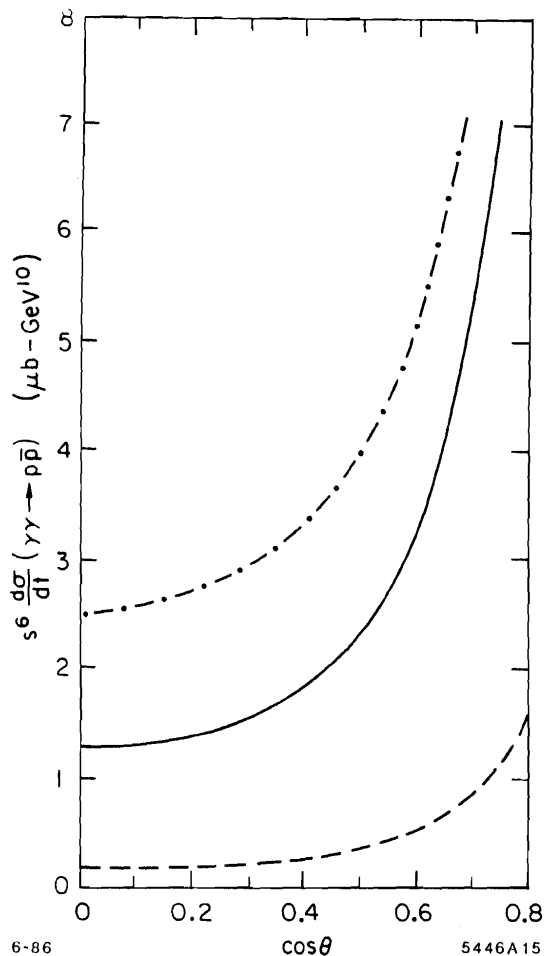


Fig. 13. QCD prediction for the scaling and angular distribution for $\gamma + \gamma \rightarrow \bar{p} + p$ calculated by Farrar et al.²⁴ The dashed-dot curve corresponds to $\frac{4\Lambda^2}{s} = 0.0016$ and a maximum running coupling constant $\alpha_s^{max} = 0.8$. The solid curve corresponds to $\frac{4\Lambda^2}{s} = 0.016$ and a maximum running coupling constant $\alpha_s^{max} = 0.5$. The dashed curve corresponds to a fixed $\alpha_s = 0.3$. The results are very sensitive to the endpoint behavior of the proton distribution amplitude. The CZ form is assumed.

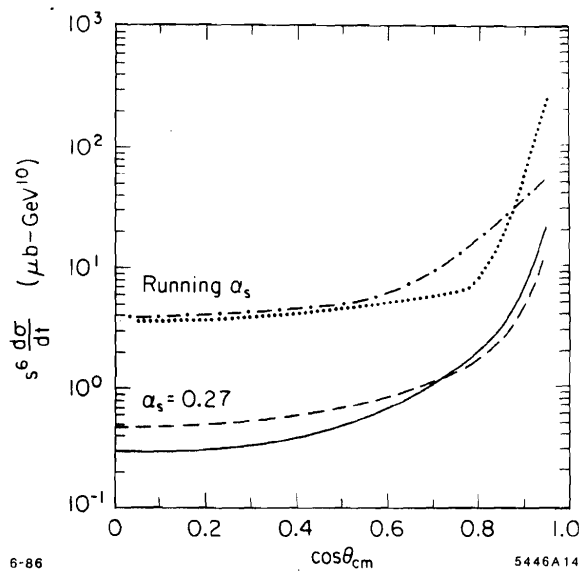


Fig. 14. QCD prediction for the scaling and angular distribution for $\gamma + \gamma \rightarrow \bar{p} + p$ calculated by Gunion, Sparks, and Millers.²⁵ CZ distribution amplitudes⁴ are assumed. The solid and running curves are for real photon annihilation. The dashed and dot-dashed curves correspond to one photon spacelike, with $\frac{Q_i^2}{s} = 0.1$.

the measured proton form factor. (See fig. 2.) The CZ sum rule analysis has been recently corrected and modified by King and Sachrajda²⁷ but the final results are not known at this time. The CZ proton distribution amplitude yields predictions for $\gamma\gamma \rightarrow p\bar{p}$ in rough agreement with the experimental normalization, although the production energy is too low for a clear test. It should be noted that unlike meson pair production²⁸ the QCD predictions for baryons are highly sensitive to the form of the running coupling constant and the endpoint behavior of the wavefunctions.

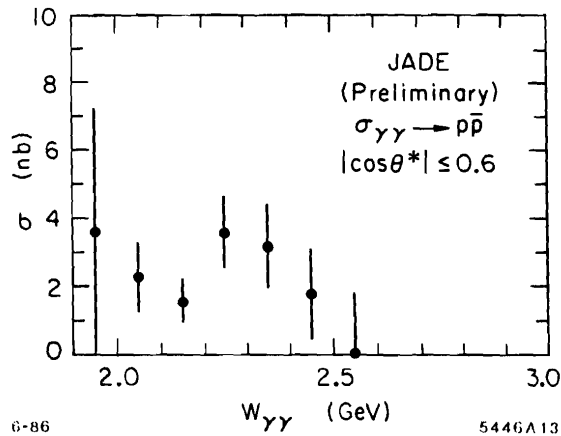


Fig. 15. Recent preliminary data from JADE²⁶ for $\gamma + \gamma \rightarrow \bar{p} + p$.

The $\gamma^*\gamma^* \rightarrow \bar{B}B$ and $M\bar{M}$ amplitudes for off-shell photons have now been calculated by Millers and Gunion.²⁹ The results show important sensitivity to the form of the respective baryon and meson distribution amplitudes. The consequences of $|gg\rangle$ mixing in singlet mesons in $\gamma\gamma$ processes is discussed in ref. 30.

It is possible that data from $p\bar{p}$ collisions at energies up to 9 GeV could greatly clarify the question of whether the perturbative QCD predictions are reliable at moderate momentum transfer.^{31,32} As emphasized in sec. 4, an important check of the QCD predictions can be obtained by combining data from $p\bar{p} \rightarrow \gamma\gamma$, $\gamma\gamma \rightarrow p\bar{p}$ with large angle Compton scattering $\gamma p \rightarrow \gamma p$. This comparison checks in detail the angular dependence and crossing behavior expected

from the theory. Furthermore in $p\bar{p}$ collisions one can even study timelike photon production into e^+e^- and examine the virtual photon mass dependence of the Compton amplitude. Predictions for the q^2 dependence of the $p\bar{p} \rightarrow \gamma\gamma^*$ amplitude can be obtained by crossing the results of Gunion and Millers.²⁹

6. Testing Hadron Helicity Conservation in $\bar{p}p \rightarrow$ Heavy Quark Resonances

The production of heavy quark resonances $p\bar{p} \rightarrow \psi, \chi, \eta_c$, etc. can be analyzed in a systematic way in QCD using the exclusive amplitude formalism of ref. 2. Since quark helicity is conserved in the basic subprocesses to leading order, and the distribution amplitude is the azimuthal angle symmetric $L_z = 0$ projection of the valence hadron Fock wavefunction, total hadron helicity is conserved for $A + B \rightarrow C + D$:²¹

$$\lambda_A + \lambda_B = \lambda_C + \lambda_D$$

The result is predicted to hold to all orders in $\alpha_s(Q^2)$. Thus an essential feature of the perturbative QCD is the prediction of hadron helicity conservation up to kinematical and dynamical corrections of order m/Q and $\langle\psi\bar{\psi}\rangle^{1/3}/Q$ where Q is the momentum transfer or heavy mass scale, m is the light quark mass, and $\langle\psi\bar{\psi}\rangle$ is a measure of non-perturbative effects due to chiral symmetry breaking of the QCD vacuum. Applying this prediction to $p\bar{p}$ annihilation, one predicts $\lambda_p + \lambda_{\bar{p}} = 0$, i.e., $S_z = J_z = \pm 1$ is the leading amplitude for heavy resonance production.²¹ Thus the ψ is expected to be produced with $J_z = \pm 1$, whereas the χ and η_c cross sections should be suppressed, at least to leading power in the heavy quark mass. The analogous tests in e^+e^- annihilation appear to be verified for ψ' decays but not the ψ . Hou and Soni³³ have suggested this effect may be due to the ψ mixing with $J = 1$ gluonium states. Antiproton-proton production of narrow resonances should be able to clarify these basic QCD issues.

7. Heavy Hadron Pair Production in $p\bar{p}$ Exclusive Reactions

One of the few areas of high energy phenomenology which is apparently not well-understood in perturbative QCD is the production of charmed hadrons. The simple fusion subprocesses $q\bar{q} \rightarrow Q\bar{Q}$ and $gg \rightarrow Q\bar{Q}$ are expected to dominate heavy quark inclusive reactions at least for very large M_Q .³⁴ However, in the case of charm production cross sections, the predictions for the energy and x_L dependence appear to contradict experiment.³⁵ It is possible that there are significant non-perturbative contributions to charm production such as the intrinsic heavy quark contributions³⁶ associated with loop interactions in the hadronic wavefunction, strong binding effects at low relative velocity,³⁷ and other non-perturbative or higher twist effects. A review of some of these issues is given in ref. 35.

Here we want to address the equally provocative question of heavy flavor production in exclusive $p\bar{p}$ reactions, e.g. $p\bar{p} \rightarrow \bar{\Lambda}_Q \Lambda_Q$ where $Q = s, c, b$. The following arguments are heuristic, but they may give a guide to the expected scaling laws and features of these reactions.

Consider the diagram of fig. 16 for the $p\bar{p} \rightarrow \bar{\Lambda}_Q \Lambda_Q$ matrix element. If the Λ 's are produced in the forward direction with $p_T^2 \lesssim \mu^2 \sim (300 \text{ MeV})^2$ then there is maximal kinematic overlap for the light quarks between the initial and final light wavefunctions. The hard subprocess cross section $\bar{u}u \rightarrow c\bar{c}$ would normally give cross sections of order

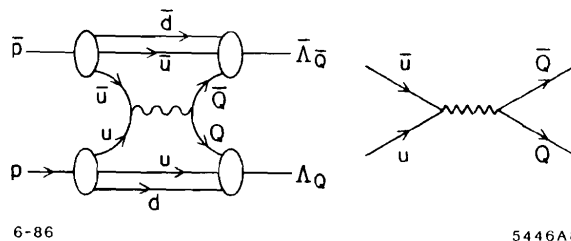


Fig. 16. Perturbative diagram for exclusive production of heavy baryon pairs in $p\bar{p}$ annihilation.

$$\frac{d\sigma}{d\Omega} \sim \frac{\alpha_s^2(s)f(\Omega)}{s} \sim \frac{\alpha_s^2(4m_Q^2)}{4M_Q^2} f(\Omega)$$

but the alignment restriction $p_T^2 < \mu^2$ gives an extra $\mu^2/4m_Q^2$ suppression in the angular integral. Therefore we expect the scaling law

$$\sigma(\bar{p}p \rightarrow \bar{\Lambda}_Q \Lambda_Q) \sim \mu^2 \frac{\alpha_s^2(4M_Q^2)}{m_Q^4} F\left(\frac{4m_Q^2}{s}\right)$$

i.e.

$$\bar{\Lambda}_s \Lambda_s : \bar{\Lambda}_c \Lambda_c : \bar{\Lambda}_b \Lambda_b = 1 : 10^{-2} : 10^{-4}$$

for $s \gg 4m_Q^2$. Thus it may not be hopeless to actually measure exclusive pairs of heavy charmed baryons in $\bar{p}p$ collisions. The above analysis can be readily extended to other heavy flavor baryon and meson pair exclusive cross sections. The issues are important for clarifying the OZI rule in QCD and the connection between exclusive and inclusive production mechanisms.

Mass corrections to QCD hard scattering amplitudes for a number of heavy quark production amplitudes have been computed. Exclusive pair production of heavy hadrons $|Q_1 \bar{Q}_2\rangle$, $|Q_1 Q_2 Q_3\rangle$ consisting of higher generation quarks ($Q_i = t, b, c$ and possibly s) can be reliably predicted³⁸ within the framework of perturbative QCD, since the required wave function input is essentially determined from nonrelativistic considerations. The results can be applied to e^+e^- annihilation, $\gamma\gamma$ annihilation, and W and Z decay into higher generation pairs. The normalization, angular dependence, and helicity structure can be predicted away from threshold, allowing a detailed study of the basic elements of heavy quark hadronization. A particularly striking feature of the QCD predictions is the existence of a zero in the form factor and e^+e^- annihilation cross section for zero-helicity hadron pair production close to a specific timelike value $q^2/4M_H^2 = m_h/2m_\ell$ where m_h and m_ℓ are the heavier and lighter quark masses,

respectively. This zero reflects the destructive interference between the spin-dependent and spin-independent (Coulomb exchange) couplings of the gluon in QCD. In fact, all pseudoscalar meson form factors are predicted in QCD to reverse sign from spacelike to timelike asymptotic momentum transfer because of their essentially monopole form. For $m_h > 2m_\ell$ the form factor zero occurs in the physical region. An interesting question is whether this type of numerator zero structure applies to the gluonic diagram amplitudes appropriate to $\bar{p}p$ reactions.

8. Exclusive Nuclear Reactions

There are a number of significant tests of QCD using \bar{p} beams in which the nuclear target itself plays an essential dynamical role.³⁹ Here we consider exclusive reactions of the type $\bar{p}d \rightarrow \gamma n$ and $\bar{p}d \rightarrow \pi^- p$ in the fixed θ_{CM} region. Dimensional counting rules predict the asymptotic behavior

$$\frac{d\sigma}{dt} (\bar{p}d \rightarrow \pi^- p) \sim \frac{1}{(p_T^2)^{12}} f(\theta_{CM})$$

since there are 14 initial and final quanta involved. One cannot expect the onset of such scaling laws until p_T is well into the multi GeV regime since each hard propagator must carry significant momentum transfer. Thus this type of scaling law is difficult if not impossible to test.

Nevertheless, there is an elegant way to test the basic QCD dynamics in these reactions using the "reduced amplitude" formalism.⁴⁰ The basic observation is that for vanishing nuclear binding energy $\epsilon_d \rightarrow 0$, the deuteron can be regarded as two nucleons sharing the deuteron four-momentum (see fig. 17). The $\bar{p}d \rightarrow \pi^- p$ amplitude then contains a factor representing the probability amplitude (i.e. form factor) for the proton to remain intact after absorbing momentum transfer squared $\hat{t} = (p - \frac{1}{2}pd)^2$ and the $\bar{N}N$ timelike form factor at $\hat{s} = (\bar{p} + \frac{1}{2}p_d)^2$. Thus

$$\mathcal{M}_{\bar{p}d \rightarrow \pi^- p} \sim F_{1N}(\hat{t}) F_{1N}(\hat{s}) \mathcal{M}_r$$

where \mathcal{M}_r has the same QCD scaling properties as quark meson scattering. We

thus predict

$$\frac{d\sigma}{d\Omega} (\bar{p}d \rightarrow \pi^- p) \sim \frac{f(\Omega)}{p_T^2} \cdot \frac{F_{1N}^2(\hat{t}) F_{1N}^2(\hat{s})}{p_T^2}.$$

The analogous analysis of the deuteron form factor as defined in

$$\frac{d\sigma}{dt} (\ell d \rightarrow \ell d) = \frac{d\sigma}{dt} \Big|_{point} (F_d(Q^2))^2$$

yields a scaling law for the reduced form factor (see fig. 18):

$$f_d(Q^2) \equiv \frac{F_d(Q^2)}{F_{1N}\left(\frac{Q^2}{4}\right) F_{1N}\left(\frac{Q^2}{4}\right)} \sim \frac{1}{Q^2}$$

i.e., the same scaling law as a meson form factor. As shown in fig. 19, this scaling is consistent with experiment for $Q = p_T \gtrsim 1$ GeV. There is also evidence^{40,41} for reduced amplitude scaling for $\gamma d \rightarrow pn$ at large angles and $p_T \gtrsim 1$ GeV. (see fig. 20). We thus expect similar precocious scaling behavior to hold for $\bar{p}d \rightarrow \pi^- p$ and other $\bar{p}d$ exclusive reduced amplitudes.

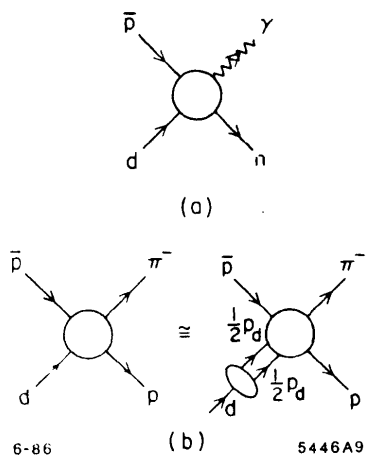


Fig. 17. Construction of the reduced nuclear amplitude for two-body inelastic deuteron reactions.⁴⁰

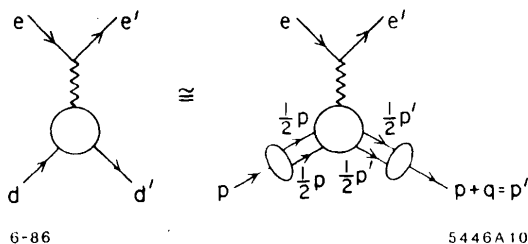


Fig. 18. Application of the reduced amplitude formalism to the deuteron form factor at large momentum transfer.

Fig. 19. Scaling of the deuteron reduced form factor. The data are summarized in ref. 40.

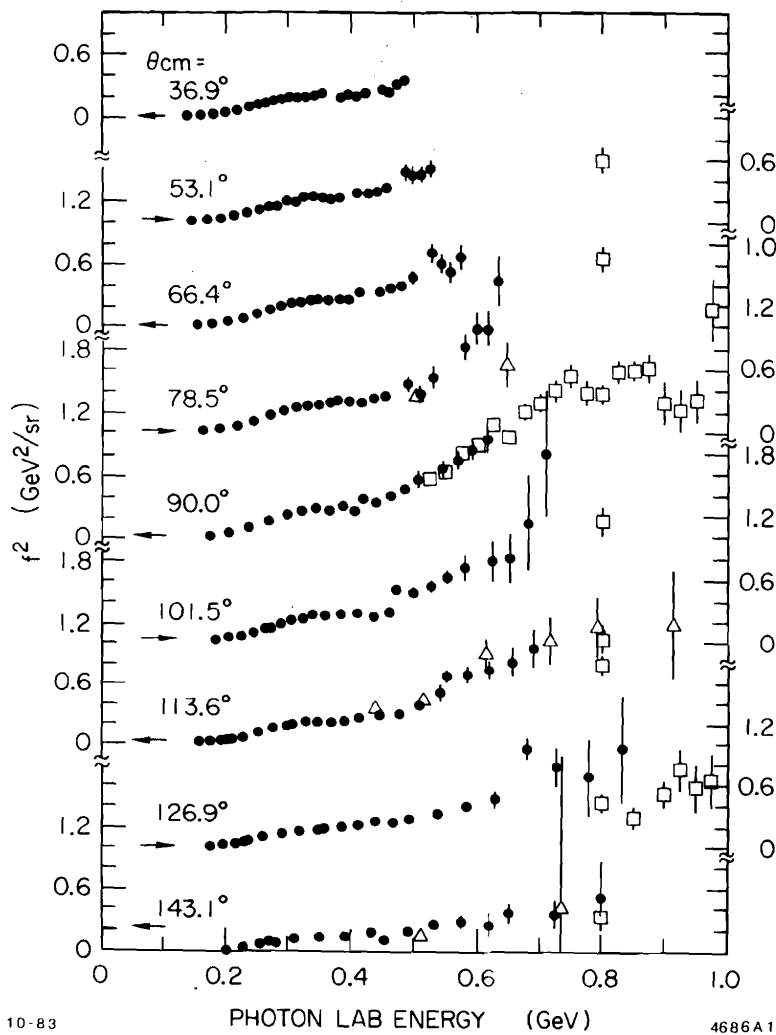
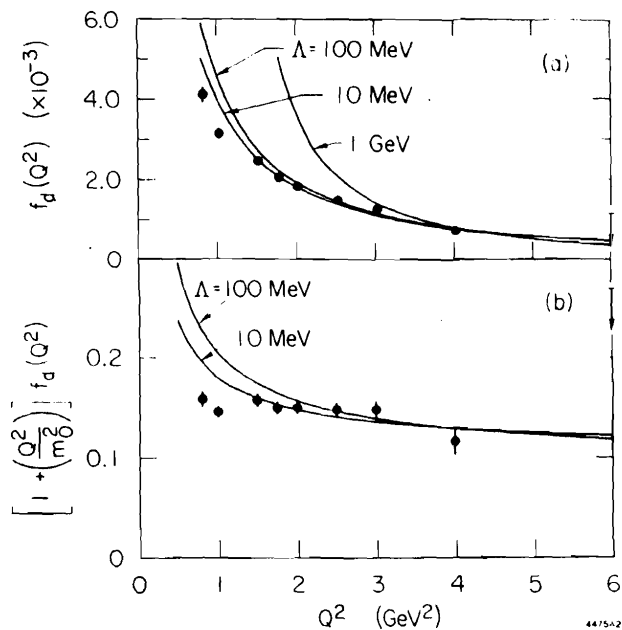


Fig. 20. Scaling of the reduced amplitude for deuteron electrodisintegration. The data are summarized in ref. 40.

9. Quasi-Exclusive Nuclear Processes

A novel feature of QCD is "color transparency" which predicts a small absorption cross section for hadrons in specific kinematic configurations.⁴² This concept can be tested in quasi-exclusive antiproton-nuclear reactions. For large p_T one predicts

$$\frac{d\sigma}{dt dy} (\bar{p}A \rightarrow \pi^+ \pi^- + (A-1)) \simeq \sum_{p \in A} G_{p/A}(y) \frac{d\sigma}{dt} (\bar{p}p \rightarrow \pi^+ \pi^-)$$

where $G_{p/A}(y)$ is the probability distribution to find the proton in the nucleus with light-cone momentum fraction $y = (p^0 + p^z)/(p_A^0 + p_A^z)$, and

$$\frac{d\sigma}{dt} (\bar{p}p \rightarrow \pi^+ \pi^-) \simeq \left(\frac{1}{p_T^2} \right)^8 f(\cos \theta_{CM}) .$$

The distribution $G_{p/A}(y)$ can be measured in $eA \rightarrow ep(A-1)$ quasi-exclusive reactions. A remarkable feature of the above equations is that there are no corrections required from initial state absorption of the \bar{p} as it traverses the nucleus, nor final state interactions of the outgoing pions. The point is that the only part of hadron wavefunctions which is involved in the large p_T reaction is $\psi_H(b_\perp \sim \mathcal{O}(1/p_T))$. i.e. the amplitude where all the valence quarks are at small relative impact parameter. These configurations correspond to small color singlet states which, because of color cancellations, have negligible hadronic interactions in the target. Measurements of these reactions thus test a fundamental feature of the Fock state description of large p_T exclusive reactions.

Another interesting feature which can be probed in such reactions is the behavior of $G_{p/A}(y)$ for y well away from the Fermi distribution peak at $y \sim m_N/M_A$. For $y \rightarrow 1$ spectator counting rules⁴³ predict $G_{p/A}(y) \sim (1-y)^{2N_s-1} = (1-y)^{6A-7}$ where $N_s = 3(A-1)$ is the number of quark spectators required to "stop" ($y_i \rightarrow 0$) as $y \rightarrow 1$. This simple formula has been quite successful in accounting for distributions measured in the forward fragmentation of nuclei at the Bevalac.⁴⁴

10. Summary

With the advent of new methods to attack non-perturbative QCD, such as sum rule constraints, implementation of effective Lagrangians such as the Skyrme model, extensions of lattice gauge theory, and promising methods to solve the light-cone Hamiltonian for its spectrum and Fock state solutions, a renaissance of interest is developing for understanding hadron and nuclear dynamics from first principles.

An experimental program with antiprotons of energies under 10 GeV can serve as an important test of QCD dynamics and the compliment to the calculational methods, especially for exclusive channels. Already there are extensive calculations available for $\bar{p}p \rightarrow \gamma\gamma$ for both real and virtual channels. Fixed angle scattering, meson-pair and lepton-pair final states also give sensitive tests of the theory. We have emphasized the possibility that the production of charmed hadrons in exclusive $\bar{p}p$ channels may have a non-negligible cross section. All of these channels bear on the question at what momentum scale perturbative factorization methods apply.

Inclusive measurements are usually studied at much higher energies than those potentially available at an AMPLE facility. Nevertheless, as discussed in sec. 3, there are interesting novel effects involving the interface between perturbative and non-perturbative dynamics and quark propagation in hadronic matter – all of which can be explored at \bar{p} energies below 10 GeV.

Finally, we have shown that \bar{p} – nuclear collisions can play an important role in clarifying fundamental QCD issues such as color transparency, critical length phenomena, and the validity of the reduced nuclear amplitude phenomenology.

Appendix A. Exclusive Reactions in QCD

In this appendix I will give a brief introduction to exclusive processes at high momentum transfer.⁴⁵ Specific applications to antiproton-initiated reactions are discussed in secs. 4-6.

The processes of interest are hadronic reactions in which all final particles are measured at large invariant masses compared with each other; this includes form factors at large spacelike or timelike momentum transfer and large angle scattering reactions such as photoproduction $\gamma p \rightarrow \pi^+ n$, nucleon-nucleon scattering at large momentum transfer, photodisintegration $\gamma d \rightarrow np$ at large angles and energies, *etc.* A crucial result is that such amplitudes factorize²⁻⁶ at large momentum transfer in the form of a convolution of a hard scattering amplitude T_H which can be computed perturbatively from quark-gluon subprocesses multiplied by process-independent "distribution amplitudes" $\phi(x, Q)^2$ which contain all of the bound-state non-perturbative dynamics of each of the interacting hadrons. An example of this factorization for meson photoproduction at large momentum transfer is shown in fig. 21. To leading order in $1/Q$ the scattering amplitude has the form

$$\mathcal{M} = \int_0^1 T_H(x_j, Q) \prod_{H_i} \phi_{H_i}(x_j, Q) [dx] \quad . \quad (A.1)$$

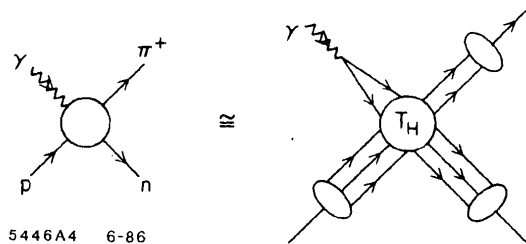


Fig. 21. Construction of the hard-scattering amplitude for pion photoproduction.

Here T_H is the probability amplitude to scatter quarks with fractional momentum $0 < x_j < 1$ from the incident to final hadron directions, and ϕ_{H_i} is the probability amplitude to find quarks in the wave function of hadron H_i collinear up to the scale Q , and

$$[dx] = \prod_{j=1}^{n_i} dx_j \delta \left(1 - \sum_k^{n_i} x_k \right) \quad . \quad (A.2)$$

The key to the derivation of this factorization of perturbative and non-perturbative dynamics is the use of the Fock basis $\{\psi_n(x_i, k_{\perp i}, \lambda_i)\}$ defined at equal $\tau = t + z/c$ on the light-cone to represent relativistic color singlet bound states. The λ_i specify the helicities; $x_i \equiv (k_i^0 + k_i^z)/(p^0 + p^z)$, ($\sum_{i=1}^n x_i = 1$), and $k_{\perp i}$, ($\sum_{i=1}^n k_{\perp i} = 0$), are the relative momentum coordinates. Thus the proton is represented as a column vector state ψ_{qqq} , ψ_{qqqg} , $\psi_{qqq\bar{q}q}$, ... In the light-cone gauge, $A^+ = A^0 + A^3 = 0$, there are no ghosts, and only the minimal "valence" Fock state needs to be considered at large momentum transfer; any additional quark or gluon forced to absorb large momentum transfer yields a power-law suppressed contribution to the hadronic amplitude. For example, at large Q^2 , the baryon form factor can be systematically computed by iterating the valence Fock state wave function equation of motion wherever large relative momentum occurs. To leading order the kernel is effectively one-gluon exchange. The sum of the hard gluon exchange contributions is the gauge invariant amplitude T_H . The residual factor from the wave function is the distribution amplitude ϕ_B which plays the role of the wave function at the origin in the analogous non-relativistic calculation. Thus we obtain the form

$$F_B(Q^2) = \int_0^1 [dy] \int_0^1 [dx] \phi_B^\dagger(y_j, Q) T_H(x_i, y_j, Q) \phi_B(x_i, Q) \quad , \quad (\text{A.3})$$

where to leading order in $\alpha_s(Q^2)$, T_H is computed from $3q + \gamma^* \rightarrow 3q$ tree graph amplitude

$$T_H = \left[\frac{\alpha_s(Q^2)}{Q^2} \right]^2 f(x_i, y_j) \quad (\text{A.4})$$

and

$$\phi_B(x_i, Q) = \int [d^2 k_{\perp}] \psi_V(x_i, k_{\perp i}) \theta(Q^2 - k_{\perp i}^2) \quad (\text{A.5})$$

is the valence three-quark wave function evaluated at quark impact separation $b_{\perp} \sim O(Q^{-1})$. Since ϕ_B only depends logarithmically on Q^2 in QCD, the main

dynamical dependence of $F_B(Q^2)$ is the power behavior $(Q^2)^{-2}$ derived from scaling of the elementary propagators in T_H . Thus, modulo logarithmic factors, one obtains a dimensional counting rule for any hadronic or nuclear form factor at large Q^2 (helicity $\lambda = \lambda' = 0$ or $1/2$)²¹

$$F(Q^2) \sim \left(\frac{1}{Q^2}\right)^{n-1} \quad (\text{A.6})$$

$$F_1^N \sim \frac{1}{Q^2}, \quad F_\pi \sim \frac{1}{Q^2}, \quad F_d \sim \frac{1}{Q^{10}}, \quad (\text{A.7})$$

where n is the minimum number of fields in the hadron. Since quark helicity is conserved in T_H and $\phi(x_i, Q)$ is the $L_z = 0$ projection of the wave function, total hadronic helicity is conserved at large momentum transfer for any QCD exclusive reaction.²¹ The dominant nucleon form factor thus corresponds to $F_1(Q^2)$ or $G_M(Q^2)$; the Pauli form factor $F_2(Q^2)$ is suppressed by an extra power of Q^2 . In the case of the deuteron, the dominant form factor has helicity $\lambda = \lambda' = 0$. The general form of the logarithmic dependence of $F(Q^2)$ can be derived from the operator product expansion at short distance or by solving an evolution equation² for the distribution amplitude computed from gluon exchange, the only QCD contribution which falls sufficiently slowly at large transverse momentum to effect the large Q^2 dependence.

The momentum scale dependence of the distribution amplitude for a baryon is determined by an evolution equation which can be derived for the Bethe-Salpeter equation at large transverse momentum projected on the light-cone:

$$\left(Q^2 \frac{\partial}{\partial Q^2} + \frac{3C_F}{2\beta}\right) \phi(x_i, Q) = \frac{C_B}{\beta} \int [dy] V(x_i, y_i) \phi(y_i, Q) \quad , \quad (\text{A.8})$$

where $C_F = (n_c^2 - 1)/2n_c = 4/3$, $C_B = (n_c + 1)/2n_c = 2/3$, $\beta = 11 - (2/3)n_f$, and $V(x_i, y_i)$ is computed to leading order in α_s from the single-gluon-exchange kernel. The evolution equation automatically sums to leading order in $\alpha_s(Q^2)$ all

of the contributions from multiple gluon exchange which determine the tail of the valence wave function and thus the Q^2 -dependence of the distribution amplitude. The general solution of this equation is

$$\phi(x_i, Q) = x_1 x_2 x_3 \sum_{n=0}^{\infty} a_n \left(\ln \frac{Q^2}{\Lambda^2} \right)^{-\gamma_n} \check{\phi}_n(x_i) \quad , \quad (A.9)$$

where the anomalous dimensions γ_n and the eigenfunctions $\check{\phi}_n(x_i)$ satisfy the characteristic equation:

$$x_1 x_2 x_3 \left(-\gamma_n + \frac{3C_F}{2\beta} \right) \check{\phi}_n(x_i) = \frac{C_B}{\beta} \int_0^1 [dy] V(x_i, y_i) \check{\phi}_n(y_i) \quad . \quad (A.10)$$

In the large Q^2 limit, only the leading anomalous dimension γ_0 contributes to the form factor.

A useful technique for solving the evolution equations is to construct completely antisymmetric representations as a polynomial orthonormal basis for the distribution amplitude of multi-quark bound states. In this way one obtains a distinctive classification on nucleon (N) and delta (Δ) wave functions and the corresponding Q^2 dependence which discriminates N and Δ form factors. The antisymmetrization technique is presented in detail in ref. 46 for nuclear systems.

The result for the large Q^2 behavior of the baryon form factor in QCD is then¹⁻³

$$G_M(Q^2) = \frac{\alpha_s^2(Q^2)}{Q^4} \sum_{n,m} d_{nm} \left(\ln \frac{Q^2}{\Lambda^2} \right)^{-\gamma_m - \gamma_n} \quad (A.11)$$

where the γ_n are computable anomalous dimensions of the baryon three-quark wave function at short distance and the d_{nm} are determined from the value of the baryon distribution amplitude $\phi_B(x, Q_0^2)$ at a given point Q_0^2 , and the normalization of T_H . The dominant part of the form factor comes from the region of the x integration where each quark has a finite fraction of the light cone momentum;

the end point region where the struck quark has $x \simeq 1$ and spectator quarks have $x \sim 0$ is suppressed by quark (Sudakov) form factor gluon radiative corrections.

The near constant behavior of $Q^4 G_M(Q^2)$ at large Q^2 (see fig. 2) provides a direct check that the minimal Fock state in the nucleon contains three quarks and that the quark propagator and the $qq \rightarrow qq$ scattering amplitudes are approximately scale-independent. More generally, the nominal power law predicted for large momentum transfer exclusive reactions is given by the dimensional counting rule $\mathcal{M} \sim Q^{4-n_{\text{TOT}}} F(\theta_{cm})$ where n_{TOT} is the total number of elementary fields which scatter in the reaction. The predictions are apparently compatible with experiment. In addition, for some scattering reactions there are contributions from multiple scattering diagrams (Landshoff contributions) which together with Sudakov effects can lead to small power-law corrections, as well as a complicated spin and amplitude phase phenomenology.^{2,47} As shown in fig. 1, recent measurements of $\gamma\gamma \rightarrow \pi^+\pi^-$, K^+K^- at large invariant pair mass are beautifully consistent with the QCD predictions²⁸ which are essentially independent of the shape of the distribution amplitude. In principle it should be possible to use measurements of the scaling and angular dependence of the $\gamma\gamma \rightarrow M^0\bar{M}^0$ reactions to measure the shape of the distribution amplitude $\phi_M(x, Q)$.²⁸ Thus far experiment has not been sufficiently precise to measure the modifications of dimensional counting rules predicted by QCD.

The actual calculation of $\phi(x, Q)$ from QCD requires non-perturbative methods such as lattice gauge theory, or more directly, the solution of the light-cone equation of motion^{2,8}

$$\left[M^2 - \sum_{i=1}^n \left(\frac{k_{\perp i}^2 + m^2}{x} \right) \right] \Psi = V_{\text{QCD}} \Psi$$

The explicit form for the matrix representation of V_{QCD} and a discussion of the infrared and ultraviolet regulation required to interpret this result is given in ref. 2.

Appendix B. QCD Sum Rule Constraints on Hadron Wave Functions

Useful constraints⁴ on the lowest moments of the distribution amplitude can be obtained using the QCD sum rule approach of the ITEP Group or by resonance saturation of vertex functions.⁴⁸ Although the numerical accuracy of these complementary methods is not known the general agreement between their predictions and overall consistency with other hadron phenomenology lends credence to their validity.

Let us first illustrate the QCD sum rule method for the case of the pion distribution amplitude. The moments $\langle x^n \rangle$ are expressible as matrix elements of gauge invariant local operators:

$$(z \cdot P)^{n+1} f_\pi \langle x^n \rangle = \langle \Omega | O_n(x) | \pi(p) \rangle \equiv \langle \Omega | \bar{d} \gamma \cdot z \gamma_5 (i z \cdot \overleftrightarrow{D})^n u | \pi(p) \rangle$$

where

$$\langle x^n \rangle = \int_{-1}^1 dx x^n \phi_\pi(x) \quad .$$

Here $x = x_1 - x_2$, $\langle x^0 \rangle = 1$, $f_\pi \cong 133$ MeV, p^μ is the pion four momentum, z^μ is a light-like vector: $z^2 = 0$, $z \cdot p = p^+$, and $\overleftrightarrow{D}_\mu = \overrightarrow{D}_\mu - \overleftarrow{D}_\mu$, where $\overrightarrow{D} = \overrightarrow{\partial}_\mu - ig A_\mu^a \cdot \frac{\lambda^a}{2}$. This relation is simplest in the gauge $z \cdot A^+ = 0$. The state $|\Omega\rangle$ is the true QCD vacuum.

In order to obtain constraints on the $\langle x^n \rangle$ one considers the correlation function between two of the O_n :

$$\begin{aligned} I_{no}(z, q) &= i \int d^4 y e^{iq \cdot y} \langle \Omega | T O_n(y) O_o(0) | \Omega \rangle \\ &= (z \cdot q)^{n+2} I_{no}(q^2) \quad . \end{aligned}$$

The "signal" between $O_o^{(0)}$ and $O_n(y)$ is carried by the pion, higher meson resonances, and the continuum. At high $q^2 \rightarrow -\infty$, $y^2 \sim \mathcal{O}(1/Q^2)$ and the operator

product expansion allows one to calculate I_{no} as an expansion in powers of $1/q^2$ involving perturbative and $\langle G^2 \rangle$ and $\langle \bar{\psi}\psi \rangle$ "vacuum condensate" contributions. On the other hand, $I_{no}(q^2)$ can be computed from a dispersion integral over hadron intermediate states. The dual identification of the power law and resonance contribution (expressed via a Borel transformation) then leads to numerical constraints on the lowest moment: The best fit obtained in ref. 4 is

$$\langle x^2 \rangle_{\pi} = 0.40, \quad \langle x^2 \rangle_{A_1} = 0.04 - 0.07$$

$$\langle x^4 \rangle_{\pi} = 0.24.$$

($\langle x^4 \rangle_{A_1}$ is small but not determined accurately.) The value of the renormalization scale μ^2 is of the order 1.5 to 2.5 GeV².

The relatively large values for the second and fourth moments imply that the pion distribution is quite broad. An additional constraint on the distribution amplitude is that ϕ vanishes at least as fast as $\phi_{\pi}^{\text{asympt}}$ at the endpoints $x \rightarrow \pm 1$. Together these constraints imply a *double-humped* distribution; the model proposed in ref. 4 is

$$\phi_{\pi}(x, \mu) = \frac{15}{4} x^2(1 - x^2) \quad .$$

There are a number of approximations which make it difficult to assess the numerical accuracy of the results. Nevertheless the distribution amplitudes derived by Chernyak and Zhitnitsky³ serve as useful forms for making QCD predictions for exclusive processes.

One of the consequences of the QCD sum rule approach is a striking dependence of the shape of the ρ -meson distribution amplitude on its helicity. This can be traced to the fact that the $\langle \bar{\psi}\psi\bar{\psi}\psi \rangle$ contribution changes sign because of the helicity dependence of the gluon-exchange interaction. A simple model for

the ρ distribution amplitude which satisfies the moment constraints is:

$$\phi^\rho(x, \mu) = \phi_{\text{asympt}}(x) \begin{cases} \frac{15}{16} x_1 x_2 & \lambda = \pm 1 \\ 1 + \frac{3}{2} \left((x_1 - x_2)^2 - \frac{1}{5} \right) & \lambda = 0 \end{cases}$$

In each case the evolution from $\mu = 500$ MeV can be computed by expanding in terms of two lowest order Gegenbauer polynomial eigensolutions. The strong helicity dependence of the ρ distribution amplitude has interesting consequences for the angular dependence of $\gamma\gamma \rightarrow \rho\rho$ cross sections.

The requirement that the nucleon is the $I = \frac{1}{2}$, $S = \frac{1}{2}$ color singlet representation of three quark fields in QCD uniquely specifies the x_i permutation symmetry of the proton distribution amplitude:

$$\begin{aligned} \phi_\uparrow^p(x_i, \mu) &\propto \frac{1}{\sqrt{6}} [d_\uparrow u_\downarrow u_\uparrow + u_\uparrow u_\downarrow d_\uparrow - 2u_\uparrow d_\downarrow u_\uparrow] \frac{1}{8} f_N [\phi_N(x_1 x_2 x_3) + \phi_N(x_3 x_2 x_1)] \\ &+ \frac{1}{\sqrt{2}} [d_\uparrow u_\downarrow u_\uparrow - u_\uparrow u_\downarrow d_\uparrow] \cdot \frac{1}{8\sqrt{3}} f_N [\phi_N(x_3 x_2 x_1) - \phi_N(x_1 x_2 x_3)] \\ &+ (1 \rightarrow 2) + (2 \rightarrow 3) \quad . \end{aligned}$$

The neutron distribution amplitude is determined by the substitution $\phi_n = -\phi_p (u \rightarrow d)$. Moments of the nucleon distribution amplitude can be computed from the correlation function of the appropriate local quark field operators that carry the nucleon quantum numbers.

The model wave function proposed in ref. 3, consistent with the derived moments, is

$$\phi_N(x_1 x_2 x_3) = \phi_{\text{asympt}} \cdot [11.35(x_1^2 + x_2^2) + 8.82x_3^2 - 1.68x_3 - 2.94 - 6.72(x_2^2 - x_1^2)]$$

where $\phi_{\text{asympt}} = 120x_1 x_2 x_3$. The renormalization scale is $\mu \cong 1$ GeV. The nor-

malization of the nucleon valence wave function is also determined:

$$f_N(\mu = 1 \text{ GeV}) = (5.2 \pm 0.3) \times 10^{-3} \text{ GeV} \quad .$$

A striking feature of the QCD sum rule prediction is the strong asymmetry implied by the first moment: 65% of the proton momentum (at $P_z \Rightarrow \infty$) is carried by the u quark with helicity parallel to that of the proton. The two remaining quarks each carry ~ 15 to 20% of the total momentum.

The striking shape of the CZ wave function is due to the fact that only the first few eigensolutions to the nucleon evolution equation are used as a basis. Since one is so far from full evolution, there is no compelling reason why this should be correct. The essential feature of the sum rule predictions is the strong asymmetry, together with the value of f_N which give perturbative predictions for the proton and neutron form factors consistent both in *sign* and *magnitude* with experiments.

Clearly the QCD sum rule wave functions have potential difficulties with endpoint singularities unless this region is strongly suppressed in T_H — *e.g.*, by the Sudakov quark form factors. A more compelling reason to be suspicious of the applicability of the QCD hard scattering formula to exclusive reactions is the striking behavior of the spin asymmetry A_N and spin correlations observed at $p_T \gtrsim 1 \text{ GeV}$ in large angle $pp \rightarrow pp$ scattering.^{20,49} However, here the theory is much more complicated than the form factor predictions, because of Landshoff pinch singularities. The strong spin dependence of baryon wave functions as indicated by the QCD sum rule approach may also be very relevant to the eventual understanding of the anomalous spin results.

References

1. For reviews see, e.g. E. Reya, Phys. Rept. 69:195, 1981; and A. H. Mueller, Lectures on perturbative QCD given at the Theoretical Advanced Study Inst., New Haven, 1985.
2. G. P. Lepage and S. J. Brodsky, Phys. Rev. D22, 2157 (1980); G. P. Lepage, S. J. Brodsky, Tao Huang, P. B. Mackenzie, CLNS-82/522, published in the proc. of the Banff Summer Institute, 1981.
3. A. H. Mueller, Phys. Rept. 73, 237 (1981).
4. V. L. Chernyak and I. R. Zhitnitskii, Phys. Rept. 112,1783 (1984). Xiao-Duang Xiang, Wang Xin-Nian, and Huang Tao, BIHEP-TH-84, 23 and 29, 1984.
5. A. V. Efremov and A. V. Radyushkin, Phys. Lett. 94B, 245 (1980).
6. S. J. Brodsky, Y. Frishman, G. P. Lepage, and C. Sachrajda, Phys. Lett. 91B, 239 (1980).
7. J. Boyer, et al., Phys. Rev. Lett. 56:207, 1986. TPC/Two Gamma Collaboration (H. Aihara, et al.), UCR-TPC-86-01, April, 1986.
8. H.C. Pauli and S.J. Brodsky, Phys. Rev. D32:1993, 1985, Phys. Rev. D32:2001, 1985.
9. S. D. Drell and T. M. Yan, Phys. Rev. Lett. 24, 181 (1970).
10. R.G. Arnold, et. al. SLAC-PUB-3810, Apr 1986.
11. S. Gottlieb, A.S. Kronfeld, Phys. Rev. D33 (1986) 227-233; CLNS-85/646, Jun 1985. 22pp.
12. G. T. Bodwin, Phys. Rev. D31:2616, 1985; G.T. Bodwin, S.J. Brodsky, G.P Lepage, ANL-HEP-CP-85-32-mc, 1985, presented at 20th Rencontre de Moriond, Les Arcs, France, Mar 10-17, 1985;
13. J. C. Collins, D. E. Soper, G. Sterman, Phys. Lett. 134B:263, 1984.
14. S. J. Brodsky, G. T. Bodwin, G.P. Lepage, in the proc. of the Volendam Multipart. Dyn. Conf. 1982:841; proc. of the Banff Summer Inst. 1981:513.. This effect is related to the formation zone principle of L.Landau and I. Pomeranchuk, Dok. Akademii Nauk SSSR 92, 535,735 (1953).
15. C.E. Carneiro , M. Day, J. Frenkel, J.C. Taylor, M.T. Thomaz, Nucl. Phys. B183:445, 1981; C. Sachrajda, Proc. of the Tahoe Multipart. Dyn. Conf. 1983:415; W.W. Lindsay, D.A. Ross, C. Sachrajda, Nucl. Phys. B222:189, 1983.

16. S.J. Brodsky, G. R. Farrar, Phys. Rev. Lett. 31:1153, 1973; Phys. Rev. D11:1309, 1975.
17. J.F. Gunion, S. J. Brodsky, R. Blankenbecler, Phys. Rev. D8:287,1973; Phys. Lett. 39B:649,1972; D. Sivers, S. J. Brodsky, R. Blankenbecler, Phys.Reports 23C:1,1976. Extensive references to fixed angle scattering are given in this review.
18. R.L. Anderson, et al, Phys. Rev. Lett. 30,627, 1973.
19. A.W. Hendry, Phys. Rev. D10:2300, 1974.
20. G.R. Court, et. al., UM-HE-86-03, Apr 1986. 14pp.
21. S. J. Brodsky, G. P. Lepage, Phys. Rev. D24:2848, 1981.
22. G. R. Farrar, RU-85-46, 1986.
23. S. J. Brodsky, C. E. Carlson, H. J. Lipkin, Phys. Rev. D20:2278, 1979; H. J. Lipkin, (private communication).
24. G. R. Farrar, E. Maina, F. Neri Nucl. Phys. B259:702, 1985, Err.-ibid. B263:746, 1986.
25. J.F. Gunion, D. Millers, K. Sparks, Phys.Rev.D33:689,1986.
26. R. Brandelik, et al., Phys.Lett.108B:67,1982. See also the proc. of the VIth Int. Workshop on Two Photon Reactions, Lake Tahoe, CA (1984), edited by R. L. Lander.
27. I.D. King, C.T. Sachrajda, SHEP-85/86-15, Apr 1986. 36pp.
28. S. J. Brodsky, G.P Lepage, Phys.Rev.D24:1808,1981. The next to leading order evaluation of T_H for these processes is given by B. Nezcic. Ph. D. Thesis, Cornell Univ. (1985).
29. D. Millers, J.F. Gunion, UCD-86-04, 1986;
30. G. W. Atkinson, N. Tsokos, and J. Sucher, Phys. Lett. 137B, 407 (1984).
31. N. Isgur and C. H. Llewellyn Smith, Phys. Rev. Lett. 52, 1080, 1984.
32. O.C. Jacob, L.S. Kisslinger, Phys. Rev. Lett. 56:225, 1986.
33. Wei-Shu Hou, A. Soni, Phys. Rev. Lett. 50:569, 1983.
34. See e.g. J. R. Cudell, F. Halzen, and K. Hikasa, MAD/PH/276 (1986), and refs. therein.
35. S. J. Brodsky, SLAC-PUB-3770, proc. of the XVI Int. Symp. on Multipart. Dyn., Tel Aviv. (1985).
36. S.J. Brodsky, P. Hoyer, C. Peterson, N. Sakai, Phys. Lett. 93B:451, 1980.

37. S. J. Brodsky, J. C. Collins, S. D. Ellis, J. F. Gunion, A. H. Mueller Published in Snowmass Summer Study 1984:227; S. J. Brodsky, J.F. Gunion, proc. of the SLAC Summer Inst. 1984:603; S. J. Brodsky H. E. Haber, J.F. Gunion, SSC/DPF Workshop 1984:100.
38. S. J. Brodsky, C.R. Ji, Phys. Rev. Lett. 55:2257, 1985.
39. See e.g. C. R. Ji , S. J. Brodsky, SLAC-PUB-3148, to be published in Phys. Rev. D; SLAC-PUB-3747, Lectures given at Stellenbosch Advanced Course in Theoretical Physics (Quarks and Leptons), Jan 21 - Feb 1, 1985; Phys. Rev. D33: 1951, 1406, 2653, (1986).
40. S. J. Brodsky and B. T. Chertok, Phys. Rev. Lett. 37, 269 (1976), Phys. Rev. D114, 3003 (1976). S. J. Brodsky and J. R. Hiller, Phys. Rev. C28, 475 (1983).
41. The data are compiled in ref. 40.
42. A. H. Mueller, proc. of the Moriond Conf. (1982); S. J. Brodsky and B. T. Chertok, ref 40; G. Bertsch, S. J. Brodsky, A.S. Goldhaber, and J. F. Gunion, Phys. Rev. Lett. 47, 297 (1981).
43. R. Blankenbecler, S. J. Brodsky, Phys. Rev. D10, 2973 (1974).
44. I.A. Schmidt, R. Blankenbecler, Phys. Rev. D15:3321, 1977.
45. The appendixes are adopted from S. J. Brodsky, SLAC-PUB-3857, proc. of the workshop on Nuclear Chromodynamics, World Scientific, eds. S. J. Brodsky and E. Moniz.
46. S. J. Brodsky and C. R. Ji, Phys. Rev. D33, 1951 (1986).
47. S. S. Kanwal, Phys. Lett. 142B, 294 (1984).
48. M.J. Lavelle, ICTP-84-85-12; Nucl. Phys. B260:323, 1985.
49. A. D. Krisch, UM-HE-85-19 (1985).